Evaluation of head response to blast using sagittal and transverse finite element head models

Dilaver Singh[1], Duane S. Cronin[2], Philip A. Lockhart[2], Tyler N. Haladuick[2], Amal Bouamoul[3], Jean-Philippe Dionne[4],
[1]*MASc Candidate, University of Waterloo, 200 University Ave West, Waterloo, ON, N2L3G1, Canada, (519) 888-4567 ext. 32309, d3singh@engmail.uwaterloo.ca*
[2]*University of Waterloo, 200 University Ave West, Waterloo, ON, N2L3G1, Canada*
[3]*DRDC Valcartier, 2459 Pie-XI Blvd North, Quebec, QC, G3J1X5, Canada*
[4]*Allen Vanguard Corporation, 2400 St Laurent Blvd, Ottawa, ON, K1G6C4, Canada*

Abstract. Blast injuries associated with exposure to Improvised Explosive Devices (IEDs) are becoming increasingly important in modern military conflicts, with mild traumatic brain injury (mTBI) reported as a significant incidence. Unlike automotive impacts, blast injuries are dominated by pressure wave dynamics, so appropriate finite element models need elements small enough to accurately model wave propagation. Although three-dimensional effects are important, the associated required mesh size results in a computationally prohibitive model. To address this, two fully coupled three dimensional slice blast-head models, in the sagittal and transverse planes, were developed using solid hexahedral elements. The head models were developed using geometry from the Visible Human Project, and were embedded in an Arbitrary Lagrangian Eulerian (ALE) mesh to simulate the surrounding air. Blast loads corresponding to 5 kg C4 at 3, 3.5, and 4 m standoffs were simulated by applying the expected pressure wave curve to the ALE mesh as a boundary condition. The brain tissue was treated as a homogeneous continuum and modeled using a linear viscoelastic constitutive model. The models were also investigated with an idealized inviscid brain material to provide an upper bound on expected strains in brain tissue. The predicted peak accelerations in both the sagittal and transverse models were in good agreement with comparable physical tests on surrogate heads, although somewhat overpredicted at the 4 m standoff. Maximum intracranial pressure values for the sagittal and transverse models were significant, ranging from 170 – 400 kPa and 200 – 300 kPa for sagittal and transverse models respectively. In general, both models reported principal strains lower than those reported for automotive crash scenarios (~0.2+). However, the strain rates were on the order of 500 s^{-1}, significantly greater than rates observed in automotive models (~10-100 s^{-1}).

1. INTRODUCTION

Blast injuries associated with exposure to Improvised Explosive Devices (IEDs) are becoming increasingly important in modern conflict zones. The increased incidence of mild traumatic brain injury (mTBI) due to blast exposure has been attributed, in part, to recent advances in traditional ballistic injury protection [1].

Blast injuries are generally divided into four classes. Primary blast injury is characterized by the interaction of the blast pressure wave with the human body, and generally affects air-containing organs such as the ears, lungs, and gastrointestinal tract. Recently, more research has focused on investigating primary blast-induced mTBI. Secondary blast injuries are due to fragmentation propelled by the blast while tertiary blast injuries are associated with the acceleration and impact of the body against a wall or the ground. Quaternary blast injuries are defined as any other related injuries such as burns, smoke inhalation, or surrounding structural collapse [2].

Charge size and standoff distance are the two primary factors affecting the load severity of the blast wave on the human body. These parameters control the peak pressure and pressure wave duration of the resulting blast where, in general, increasing standoff distance results in lower peak pressures and longer durations. Predicting brain injury due to blast loads is challenging due to both the complex nature of the loading, as well as a limited understanding of brain injury mechanisms. Unlike automotive or sports related impacts, primary blast injuries are related to pressure wave dynamics, so that finite models used to investigate this phenomenon require elements small enough to accurately model wave propagation. Although three-dimensional (3D) effects are important, the associated required mesh size results in a computationally prohibitive model. To address this, two fully coupled 3D slice blast-head models, in the sagittal and transverse planes, were developed using solid hexahedral elements. Solid elements were required because of the use of the ALE formulation in LS-DYNA. This study compares the two finite

element models under blast load conditions to evaluate global and local response of the head, and investigate potential for injury.

2. BACKGROUND

2.1 Head Injury

A significant challenge in impact biomechanics is correlating measured tissue response to a probability of injury. For head and brain injuries, this challenge is compounded by the difficulty of experimental testing *in vivo*, as well as a limited understanding of brain injury mechanisms. The human brain is a complex organ composed primarily of neurons and neuroglia. Brain tissue has been shown to exhibit nearly incompressible, viscoelastic material behaviour, as well as regional variation in stiffness and regional anisotropy [3]. The brain is separated from the skull by three membranes called meninges, and surrounded by the cerebrospinal fluid (CSF) for protection against mechanical shock [4].

One method of evaluating injury is by comparing the stress and strain response of the tissue to established injury thresholds. Various stress and strain thresholds have been proposed by different authors as potential injury metrics. Intracranial pressure is a commonly used brain injury metric in the literature, although the proposed injury threshold values vary significantly from different authors. Kleiven proposed 66 kPa for a 50% probability of concussion [5] while Zhang *et* al. proposed 90 +/- 24 kPa for mTBI based on data from NFL collisions [6] whereas Ward *et* al. used numerical models to predict that a peak intracranial pressure of 234 kPa could result in serious brain injury, although this research used a relatively coarse mesh (~10 mm) and simplified material properties which may undermine the validity of this threshold [7].

Another common brain injury metric is first principal strain. Wayne State University concluded that a peak principal strain of 0.121 indicated axonal damage, based on research conducted on rats [8]. Kleiven proposed that a principal strain of 0.21 corresponded to 50% probability of concussion [5] while Deck *et* al. reported a threshold principal strain of 0.40 for severe diffuse axonal injury [9]. Other studies by Bayly and Feng have investigated measuring strain fields in human test subjects during mild frontal and occipital head impacts [10, 11]. In a previous study, maximum shear stress was found to not be a significant factor in the injury response to a blast load [12].

An alternative method for evaluating brain injury are the overall head kinematics in terms of head acceleration (linear and/or rotational). In general, the head can withstand higher accelerations over shorter durations. However there is currently no consensus for acceleration thresholds that are relevant to the much shorter durations associated with blast loading. The automotive industry has developed criteria for predicting head injury in vehicle crash scenarios. The most widely used of such criteria is the Head Injury Criterion (HIC). The HIC calculates a time integral of the total linear acceleration of the head, as shown in Equation 1 [13]. HIC tolerance limits of 700 and 1000, for 15 ms and 36 ms calculation time windows respectively, are used in the automotive industry [13, 14]. HIC has been used in previous studies for evaluating blast injury to soft tissue from antipersonnel mines [15, 16].

$$\mathrm{HIC} = \left[\frac{1}{(t_2 - t_1)} \int_{t_1}^{t_2} a(t)\,dt\right]^{2.5} (t_2 - t_1) \tag{1}$$

Gennarelli *et* al. proposed another criterion for head injury that uses rotational velocity and acceleration to define injury thresholds [17]. More recently, another criterion called the Head Impact Power (HIP) has been proposed, which uses information from American football games to define injury thresholds based on total power input to the head, including both rotational and linear acceleration [18]. However, both the rotational criterion and the HIP have been found to produce results comparable to HIC for blast load scenarios [14], and thus were not considered in this study.

2.2 Blast Load Physics

When typical high explosives (HE) such as C4 or TNT detonate, the solid explosive material is rapidly converted into high pressure gases, which expand into the surrounding air. In a free-air detonation, this expansion creates a fireball that expands and subsequently contracts, as well as a supersonic pressure shock wave that propagates outwards from the charge centre [19]. Primary blast injuries are associated with the interaction between this pressure wave and the human body. Figure 1 is an idealized pressure profile for a

blast wave, called the Friedlander curve [20]. It consists of a positive pressure phase, followed by a negative pressure phase caused by the expansion and contraction of the fireball.

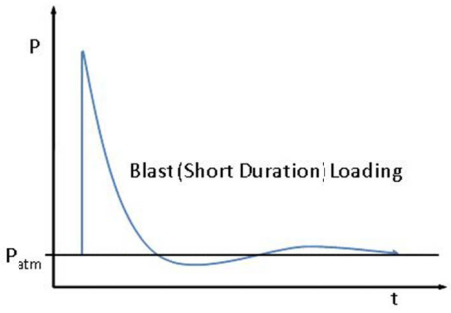

Figure 1: Friedlander curve [20]

Blast overpressure is defined as the rapid rise in ambient pressure as a result of the blast, and is generally considered to be the peak pressure in the Friedlander curve. For conventional HE at typical standoffs, the positive phase durations are on the order of milliseconds [21]. Blast overpressure can be related to temperature and specific volume using the Rankine-Hugoniot relations for air, shown in Equations 2 and 3 [22].

$$\text{temperature} = T = T_0 \left(\frac{7+\frac{\Delta P}{P_0}}{7+6\frac{\Delta P}{P_0}} \right) \left(1 + \frac{\Delta P}{P_0} \right) \tag{2}$$

$$\text{specific volume} = \frac{v}{v_0} = \frac{7+\frac{\Delta P}{P_0}}{7+6\frac{\Delta P}{P_0}} \tag{3}$$

There are two distinct measures of pressure that need to be distinguished in regards to blast waves: static pressure and dynamic pressure. Static pressure, also called incident or side-on pressure, is the pressure experienced by a particle within the flow itself. Incident pressure is more commonly used as a reference in experimental testing. Dynamic pressure is related to the kinetic energy of the fluid and its interaction with a structure. When a pressure wave collides with a surface, some of it is reflected back and interacts with the incoming wave, causing the surface to experience a greater pressure force called the reflected pressure [22].

3. METHODS

3.1 Finite Element Model

An explicit finite element code (LS-DYNA), which has been extensively used for numerical simulation of explosive detonation and subsequent interaction with the human body [23], was used for this study. By definition primary blast injury is exclusively dominated by pressure wave dynamics and an appropriate model must accurately simulate shock wave propagation and include an appropriately refined finite element mesh. A complete 3D head model with the required level of mesh refinement and continuity between structures was deemed computationally prohibitive, discussed below, and solid slice models were developed.

The detailed head model geometries were derived from the Visible Human Project (VHP) male data set (Figure 2) [24]. The sagittal model used in this study was originally developed by Lockhart [22], and the transverse model was originally developed by Cronin *et* al. [14]. The average element size requirement of 1 mm was determined by Lockhart from a grid convergence study of the sagittal model, in agreement with existing literature [22, 25]. The average element size of both the sagittal and transverse models used in this study was 1 mm.

The head models were composed of 3D hexahedral elements, which are recommended for computational accuracy, particularly for modeling wave phenomena and blast loads [26]. An arbitrary Lagrange Eulerian (ALE) formulation was used to model the air surrounding the head models and to apply

the blast loading so that this was a fully coupled analysis. This method also accounts for the large deformations in the air elements caused by the blast wave. The dimensions of the air mesh were 1.2 m x 2.05 m, in order to eliminate any boundary reflections which may have interfered with the simulation. The element size of the air elements near the head models was 1 mm, to ensure wave interaction with the models was accurate, as well as to maintain similar element sizes between the Lagrangian and Eulerian elements to facilitate coupling. A graded mesh was used to reduce computation time away from the region with the head (Figure 3).

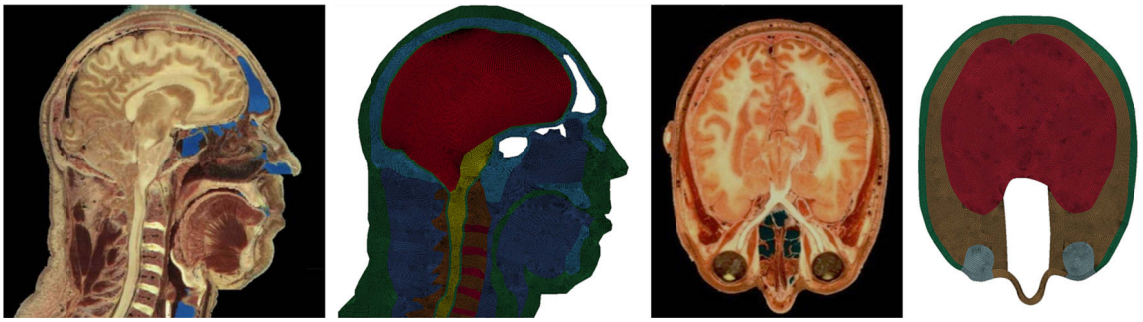

(a) (b)

Figure 2: Visible Human Project images and head FE models for *(a)* sagittal and *(b)* transverse planes [24]

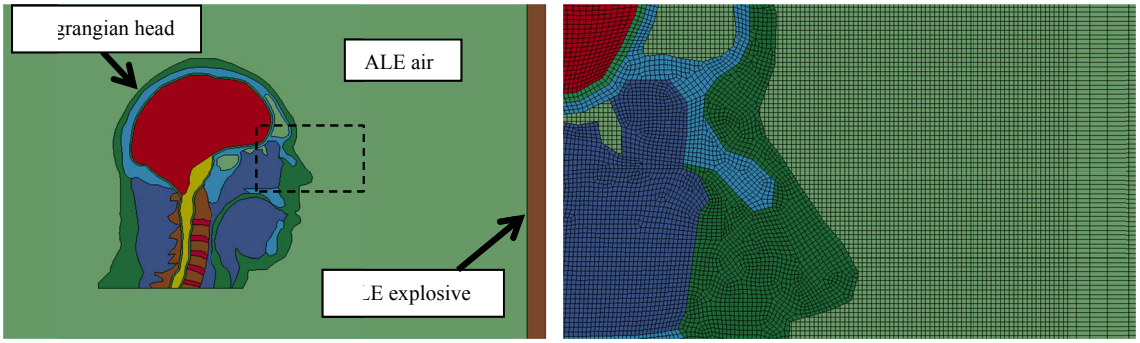

Figure 3: Embedded head model in ALE air mesh with close-up (inset)

To ensure accurate propagation of pressure waves within the head models, elements between adjacent tissue layers were joined, creating a continuous mesh. It has been noted that this could affect the shear stress and strain behaviour of the models, especially near the CSF where there may be significant sliding motion. However, since the strains observed in the models were smaller than those typical in automotive scenarios, and previous simulations with contact interfaces demonstrated no significant difference in results, this boundary condition was found to be reasonable [27]. All nodes in the head models and the air mesh were constrained from out-of-plane rotation and translation. Furthermore, the bottom layer of nodes at the neck of the sagittal model was fully constrained in order to capture rotational acceleration caused by the neck/torso interface.

3.2 Tissue Material Properties

Appropriate constitutive material properties were assigned to each tissue component in the models. The material parameters used for this study were based on the parameters proposed by Lockhart [22] (Table 1). The hyperelastic material model for the muscle and soft tissue was defined by a series of uniaxial stress-strain curves at different strain rates based on the work of van Sligtenhorst [28]. The sinuses and nasal cavities were approximated as air, and filled with ALE air elements. The skull, vertebrae, vertebral discs, and skin were modeled as elastic materials since tissue failure or fracture was not anticipated, and the cerebrospinal fluid was modeled as a fluid.

For the current study, the brain tissue was treated as a homogeneous continuum and modeled using a linear viscoelastic constitutive model. Previous studies have deemed this approximation of brain tissue to be acceptable by comparison with experimental data [29]. The literature contains a range of proposed viscoelastic material constants for brain tissue (Table 2). In order to treat the brain as a homogeneous

continuum, values for different regions of the brain were averaged into a single value. A small side study demonstrated that the effect of this averaging on the model response was not significant.

The tissue response in the models was also investigated with a viscous material model with bulk properties similar to those of water (Table 2). The viscosity was set to that of water, providing minimal resistance to dynamic shear, and thus provided maximum predicted strains for a particular load case. This effectively provided an upper bound on expected strains in the brain tissue under the tested blast load conditions.

Table 1: Constitutive material properties for tissue materials, from Lockhart [22]

Tissue	*Material Model*	*Density (kg/m^3)*	*Poisson's Ratio*	*Young's Mod. (Pa)*	*Bulk Mod. (Pa)*	*G_0 (Pa)*	*G_∞ (Pa)*	*B (s^{-1})*
Skull/Vertebrae [14]	Elastic	1561	0.379	7.92e9				
Vertebral Discs [30]	Elastic	1040	0.40	1.7e9				
Skin [14]	Elastic	1200	0.42	3.4e9				
Muscle/Soft Tissue [28, 31]	Hyperelastic	1050			2.2e9			
CSF [31]	Fluid	1040			2.2e9			
Brain/Spinal Cord	Linear Viscoelastic	1050			2.2e9	49000	16200	145

Table 2: Constitutive material properties for brain tissue

Literature Source	*G_0 (Pa)*	*G_∞ (Pa)*	*B (s^{-1})*	*Viscous Fluid Material Properties*
Takhounts [32]	1662	928	16.95	Density = 1050 kg/m3
Zhu [33]	15900	3600	504.5	Dynamic viscosity = 8.90e-4 Pa·s
Zhang [34]	44333	7333	400	Gruneisen EOS parameters [36]:
Ipek [35]	49000	16200	145	C = 1483, S1 = 1.75, γ = 0.28

3.3 Blast Load Modeling

To model a physically realistic blast wave to the head models, a one element thick strip of unique ALE elements was created on the leading edge of the air mesh (Figure 3). The specific volume and temperature histories for these elements were then defined as a boundary condition, to simulate the blast pressure wave from an explosive detonation. This simulated blast wave propagated through the ALE air mesh and interacted with the head models. The use of an ALE air mesh allowed for complex blast wave interactions with the head models to be simulated. This method of modeling blast loads has been used in previous studies and validated against experimental data [14, 22].

This study considered three blast load cases; a 5 kg charge of C4 high explosive with standoff distances of 3, 3.5, and 4 m. The detonations were modeled as free-air spherical bursts with no surface or ground interaction. The pressure curve profiles for each load case were extracted from LS-DYNA using the Conventional Weapons (CONWEP) formulations [23]. The CONWEP equations use the charge size and standoff distance to predict reflected pressures due to a blast on a flat surface. The pressure curves from CONWEP were converted to temperature and specific volume histories using the Rankine-Hugoniot equations (Eq. 2 and Eq. 3) and applied to the leading edge of the ALE air elements.

4. RESULTS

4.1 Pressure Wave Dynamics

Pressure fringe plots for the sagittal and transverse models with the surrounding ALE mesh for a 4 m standoff distance are shown in Figure 3. Both models demonstrated complex pressure wave interaction with the head geometries. In the transverse model, the pressure wave enveloped the head and created a strong pressure field at the back of the head, although the similar effect in the sagittal model was a result of the neck boundary condition. Pressure waves propagating in the brain were also observed in both models, showing how the initial blast wave transmitted though the facial tissue and then into the brain. Skull flexure, on the order of less than 1 mm, was observed in both models as a structural response to blast, however the significance of skull flexure as an injury mechanism is unclear.

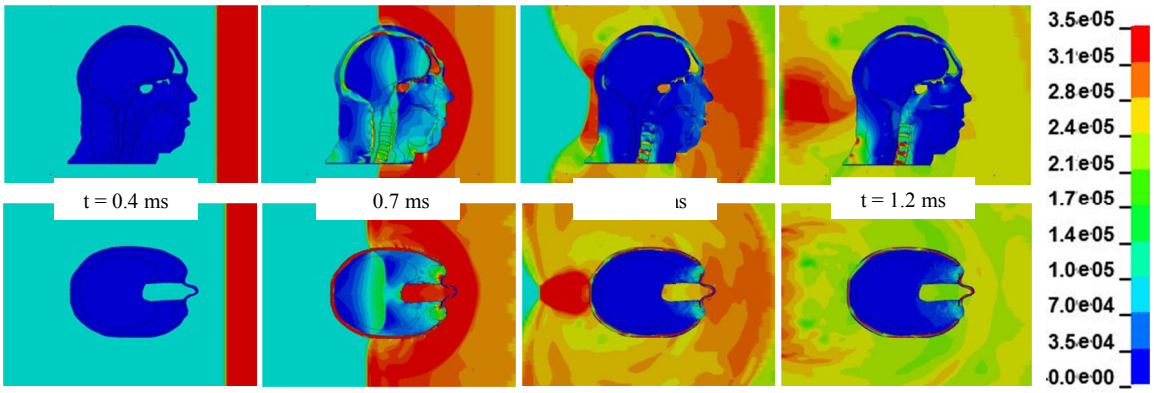

Figure 3: Pressure (Pa) fringe plot histories of sagittal and transverse models for 4 m standoff

4.2 Constitutive Model Analysis

The maximum first principal strains of the sagittal and transverse models for various constitutive models for 4 m standoff are shown in Figure 4. The response of the fluid material is also shown and as expected, predicts the greatest strains for both models. The transverse model with the fluid material model predicted non-physical values of strain at two locations attributed to the mesh configuration, which were not included in the results. The maximum principal strains for the 4 m standoff predicted in the brain tissue by the null material were 0.12 for the sagittal and 0.55 for the transverse model. The greater strain response in the transverse model was attributed to the relatively low amount of facial tissue protecting the brain in the transverse slice considered for this model. The different linear viscoelastic constitutive parameters predicted maximum strains that increased in accordance with their shear moduli. The maximum effective strain rates for different constitutive models at 4 m standoff are shown in Figure 5. The strain rates did not differ significantly with the constitutive parameters; however the fluid material model predicted considerably greater strain rates: 4512 s^{-1} for the sagittal and 1557 s^{-1} for the transverse model.

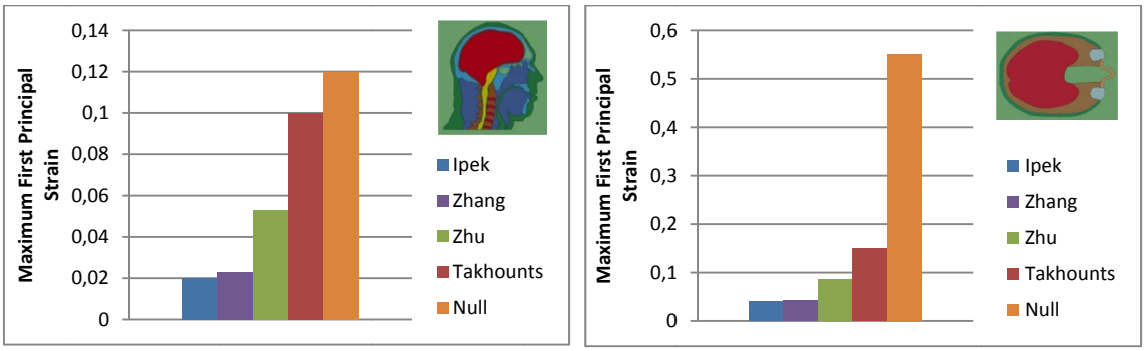

(a) (b)

Figure 4: Maximum strains for constitutive models in *(a)* sagittal and *(b)* transverse planes at 4 m standoff

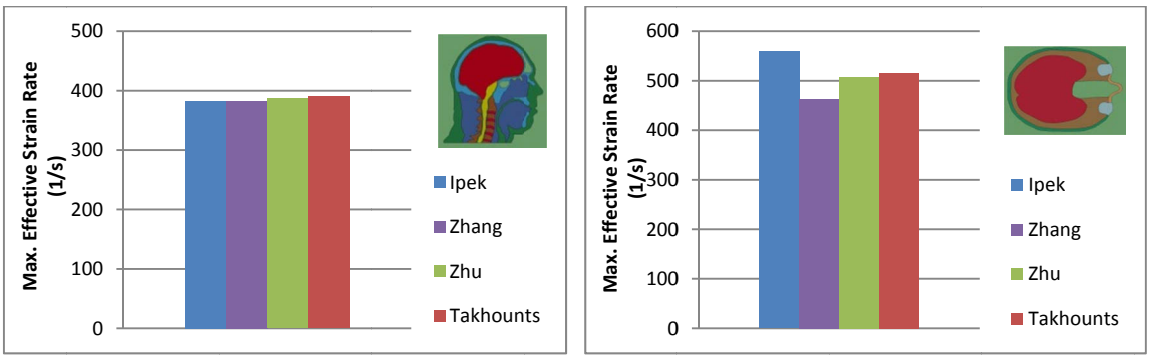

(a) (b)

Figure 5: Max strain rates for constitutive models in *(a)* sagittal and *(b)* transverse planes at 4 m standoff

4.3 Brain Tissue Response

The constitutive material parameters from Zhu *et* al. [33], providing average strain response (Figure 4) were used for subsequent studies. The local brain tissue response of the head models was evaluated based on first principal strain, and positive and negative intracranial pressure. For clarity, this data is presented in plots showing the volume fraction of the brain exposed to maximum values of pressure or strain, over the course of the simulation.

The first principal strain data for the sagittal and transverse models are shown in Figure 6. The maximum principal strains reported by the sagittal model for 4, 3.5, and 3 m standoffs were 0.053, 0.054, and 0.087. The corresponding maximum strains for the transverse model were 0.085, 0.087, and 0.15. Bayly *et* al. reported maximum principal strains of 0.05 to 0.06 for mild frontal and occipital head impacts on live human test subjects, however the head accelerations in these tests ranged from 2 - 3 g over 40 – 56 ms, whereas accelerations caused by blasts are on the order of several hundred g in under 1 ms [10]. The automotive finite element head model by Takhounts *et* al. reported a maximum principal strain of 0.347 with 135 g of peak linear acceleration [32]. Overall, the principal strains predicted by the models under blast are relatively low compared to automotive models and traditional impact methods [9, 37].

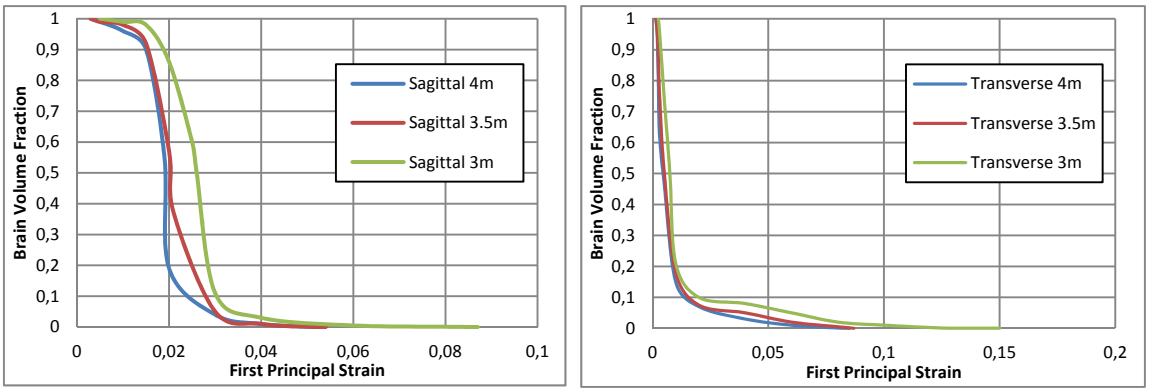

(a) (b)

Figure 6: First Principal strain for *(a)* sagittal and *(b)* transverse models for various standoffs

The maximum effective strain rates ranged from 378 – 521 s^{-1} for the sagittal model and 369 – 578 s^{-1} for the transverse model, depending on the standoff distance. Strain rates on this order of magnitude are expected in blast loads because of the extremely short durations of the loading, and are in agreement with the literature [38, 39].

The positive intracranial pressure data for the sagittal and transverse models are shown in Figure 7. As expected, a higher volume fraction of the brain was exposed to greater intracranial pressures as the standoff distance decreased; however this relationship was more noticeable in the sagittal model. The maximum intracranial pressures values were comparable for both models, although the sagittal model reported greater values for lower standoffs.

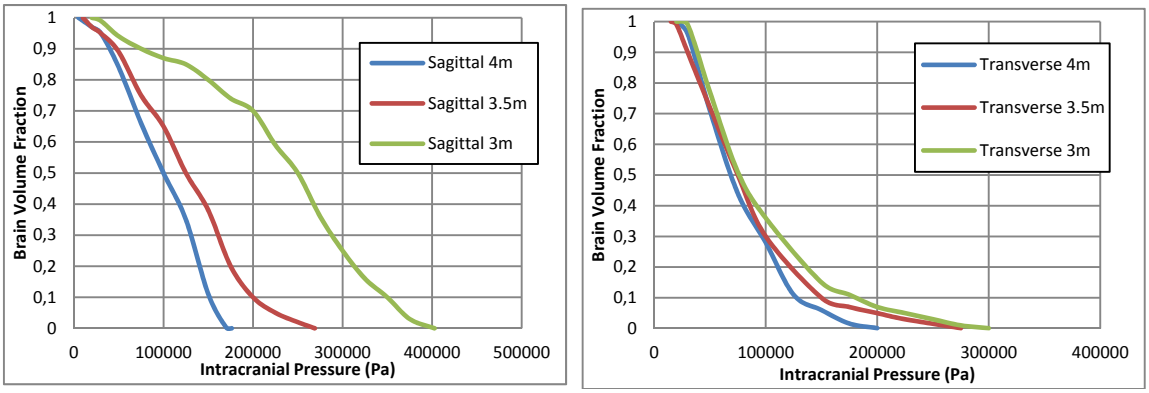

(a) (b)

Figure 7: ICP for *(a)* sagittal and *(b)* transverse models for various standoffs

Figure 8 shows the data for negative intracranial pressure for both models. The models were comparable in terms of maximum negative pressure for the 3 m and 3.5 m standoffs, however the transverse model predicted a greater value for the 4 m standoff. Overall, the values of maximum negative pressure were similar to the values of maximum positive pressure, on the order of several atmospheres. Both models predicted the greatest positive pressures at the anterior of the brain and the greatest negative pressures on the posterior, suggesting the possibility of a coup, contre-coup type injury.

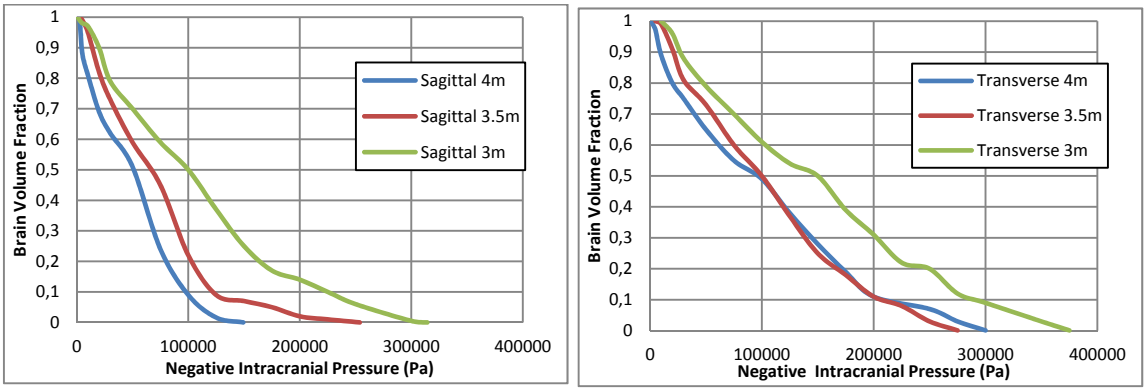

(a) (b)

Figure 8: Negative ICP for *(a)* sagittal and *(b)* transverse models for various standoffs

4.4 Head Kinematics

This study compared the peak accelerations of the head models with a simplified rigid body numerical model of a human called the Generator of Body Data (GEBOD), as well as experimental data conducted by Defense Research and Development Canada (DRDC) on a Hybrid III crash test dummy head [40]. The acceleration response of the quasi-2D slice models was measured at the node corresponding to the centre of gravity for each model. All acceleration data was filtered using a CFC1000 filter [22]. The HIC_{15} values for each load case were calculated in LS-DYNA using the acceleration response curves.

The peak accelerations and HIC_{15} values are shown for all three standoffs in Figure 9. Peak acceleration values expectedly decreased as standoff distance increased. The accelerations for the numerical models were in good agreement with each other, although somewhat overpredicted the response at the 4 m standoff compared to the experimental data. The HIC_{15} values for the numerical models were also in good agreement with each other, and fell within the scatter of experimental data for the 4 m standoff; however they are overpredicted for the 3 m and 3.5 m standoffs. Using the HIC_{15} threshold of 700, injury may be predicted for the 3.5 m and 3 m standoffs, although the validity of using the automotive HIC_{15} in a blast scenario with very short duration loading is uncertain.

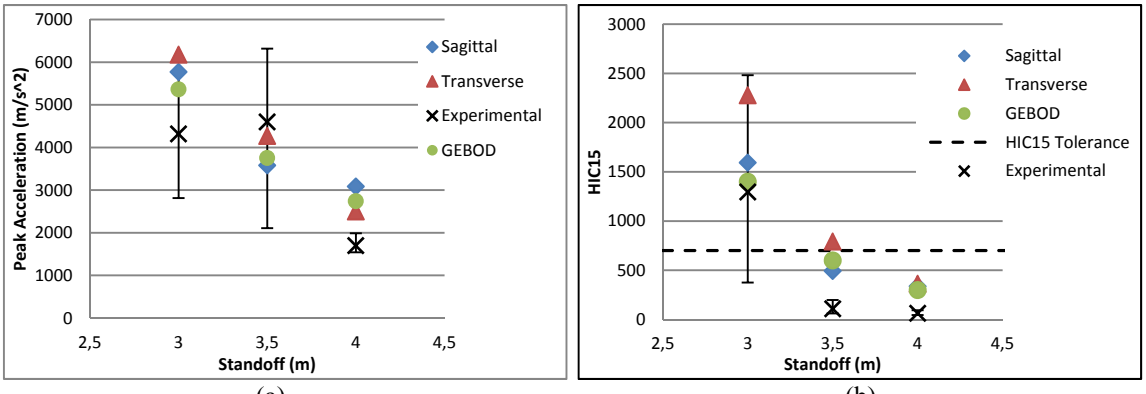

(a) (b)

Figure 9: *(a)* Peak linear acceleration and *(b)* HIC_{15} of models for various standoffs

5. CONCLUSIONS

This study compared two detailed finite element head models in three blast load cases, in terms of brain tissue response and head kinematics. In general, both the sagittal and transverse models predicted principal strains lower than those seen in automotive crash scenarios. However, the strain rates were on the order of 500 s^{-1}, significantly greater than rates observed in automotive models. In typical automotive impacts, principal strains of 0.20 and greater, at rates of 10 – 100 s^{-1} are common [9, 37]. The models were also investigated with an idealized inviscid, or fluid, brain material to provide an upper bound on expected strains in brain tissue under blast loads. For the 4 m standoff, the models with the fluid material reported maximum strains of 0.12 and 0.55 for the sagittal and transverse respectively.

Maximum intracranial pressure values for both models were significant, ranging from 170 – 400 kPa in the sagittal mode, and 200 – 300 kPa in the transverse, depending on the standoff. Maximum negative pressures in the brain volume were similar in magnitude. Both models reported greatest positive pressures on the anterior of the brain, and greatest negative pressures on the posterior, suggesting the possibility of coup, contre-coup injury.

The predicted peak accelerations in both the sagittal and transverse models were in good agreement with each other as well as the numerical Generator of Body Data (GEBOD) model, although the accelerations were overpredicted for the 4 m standoff compared to experimental data. The HIC_{15} values for both models were overpredicted for the 3.5 m and 4 m standoffs, but fell within the scatter of experimental data for the 3 m standoff. Both models exceeded the HIC_{15} tolerance of 700 for the 3 m standoff, only the transverse model exceeded it for the 3.5 m standoff, and neither model exceeded this threshold for the 4 m standoff. Although the HIC_{15} provides a useful benchmark for comparing the data, it should be noted that the HIC was developed for the automotive industry for loads with much longer durations than blast loads.

A limitation of this study is that complex 3D wave interactions were not considered. Furthermore, most of the injury criteria available in the literature have not been developed for evaluating blast loads, so the relationship between tissue response and injury is still under investigation. Importantly, these models have allowed us to associate increasing tissue response with increased blast load severity and quantify the expected strains and strain rates experienced in brain tissue, which can be used to guide future material characterization.

Acknowledgements
The authors would like to acknowledge the support of the Natural Sciences and Engineering Research Council, Defence Research and Development Canada – Valcartier, and Allen Vanguard Corporation.

References

[1] Connolly T.J.M. and Clutter J.K., Safety Science, 48 (2010), 1387-1392.
[2] Gruss E., Journal of Neurotrauma, 60 (2006), 1284-1289.
[3] Prange M.T. and Margulies S.S., Journal of Biomechanical Engineering, 124 (2002), 244-252.
[4] Schmitt K.U. *et* al, Trauma biomechanics – accidental injury in traffic and sports, 3rd edition (Springer, New York, NY, 2010).
[5] Kleiven S., Biomechanics and thresholds for MTBI in humans, MTBI Pre-Congress Symp., Lisbon, Portugal, 2008.
[6] Zhang L. *et* al., Journal of Biomechanical Engineering, 126 (2004), 226-236.
[7] Ward C. *et* al., Intracranial pressure – a brain injury criterion, Proc. 24th Stapp Car Crash Conf., Troy, MI, October 1980, pp. 163-185.
[8] Mao H., Computational analysis of in vivo brain trauma, Collection for Wayne State Univ., 2009.
[9] Deck C., and Willinger R., International Journal of Crashworthiness, 13 (2008), 667-678.
[10] Bayly P.V. *et* al., Journal of Neurotrauma, 22 (2005), 845-856.
[11] Feng Y. *et* al., J. R. Soc. Interface, 7 (2010), 1677-1688.
[12] Singh D. *et* al., Comparison of detailed sagittal and transverse finite element head models to evaluate blast load response, IASTED Biomech, Pittsburgh, PA, November 2011.
[13] Hutchinson J. *et* al., Applied Mathematics and Computation, 96 (1998), 1-16.

[14] Cronin D.S., Salisbury C., *et* al., Numerical modeling of blast loading to the head, Proc. PASS, Brussels, Belgium, 2008, 84-93.
[15] Makris A., Nerenberg J., Dionne J.P., *et* al, Reduction of Blast Induced Head Acceleration in the Field of Anti-Personnel Mine Clearance, Med-Eng Systems Inc, Ontario, CA, 2000.
[16] Dionne J.P., Nerenberg J., and Makris A., Reduction of Blast-Induced Concussive Injury Potential and Correlation With Predicted Blast Impulse, Med-Eng Sys. Inc, Ontario, CA, 2002.
[17] Gennarelli T.A. *et* al., Ann. Proc. Assoc. Adv. Automot. Med., 47 (2003), 624-628.
[18] Newman J.A. *et* al., A proposed new biomechanical head injury assessment function, Proc. 44th Stapp Car Crash Conf., Atlanta, GA, 2000, OOS-80.
[19] Hetherington J.G. and Smith P.D., Blast and ballistic loading of structures (Butterworth-Heinemann, Burlington, MA, 1994).
[20] Thom C.G. and Cronin D.S., Blast loading amplification and attenuation by fabric materials and the effect of primary blast injury, Proc. PASS, Quebec City, Canada, 2010.
[21] Kingerey C.N. and Bulmash G., Airblast parameters from TNT spherical air burst & hemispherical surface burst, Tech Report ARBRL-TR-02555, 1984.
[22] Lockhart P.A., Primary blast injury of the head: Numerical prediction and evaluation of protection, MASc Thesis, Waterloo, Canada, 2010.
[23] Hallquist J.O., LS-DYNA Theory Manual, Livermore, CA, 2006.
[24] Visible Human Project, U.S. National Library of Medicine, NIH
[25] Greer A., Numerical modeling for the prediction of primary blast injury to the lung, MASc Thesis, Waterloo, Canada, 2006.
[26] Puso M.A. and Solberg J., Int. Journal for Numerical Methods in Engineering, 67 (2006), 841-867.
[27] Chafi M.S. *et* al., Annals of Biomedical Engineering, 38 (2010), 490-504.
[28] van Sligtenhorst C., Cronin D.S., Brodland G.W., Journal of Biomechanics, 39 (2006), 1852-1858.
[29] Wittek A. and Omori K., JSME Int. Journal, 46 (2003), 1388-1399.
[30] Kleinberger M., Application of finite element techniques to the study of cervical spine mechanics, Proc. 37th Stapp Car Crash Conf., San Antonio, TX, 1993.
[31] DuBois P.A., A simplified approach to the simulation of rubber-like materials under dynamic loading, 4th European LS-DYNA Users Conference, 2003.
[32] Takhounts E.G. *et* al., Stapp Car Crash Journal, 52 (2008), 1-31.
[33] Zhu F. *et* al., Materials & Design, 31 (2010), 4704-4712.
[34] Zhang L. *et* al., Journal of Neurotrauma, 18 (2001), 21-30.
[35] Ipek H. *et* al., Coupling of Strasbourg University head model to THUMS human body FE model: Validation and application to automotive safety, 2009, 1-13.
[36] Tan P. *et* al., FEA modelling prediction of the transmitted overpressure and particle acceleration within a frame subjected to shock tube blast loadings, IMACS, Australia, July 2009, 1657-1663.
[37] Danelson K. *et* al., Stapp Car Crash Journal, 52 (2008), 59-81.
[38] Shafieian M. *et* al., Mechanical properties of brain tissue in strain rates of blast injury, J. Cerebral Blood Flow and Metabolism, 2011, 4-5.
[39] Sista B., and Vemaganti K., Modeling and Simulation of the High Strain-Rate Response of Brain Tissue for Traumatic Brain Injury Applications, Ohio State Univ. Biomech. Symp., 2011.
[40] Haladuick T.N. *et* al., Modelling of global head kinematics resulting from realistic blast loading, IASTED Biomech, Pittsburgh, PA, November 2011.